4th URSI AT-RASC, Gran Canaria, 19-24 May 2024

Development of Absolute Quantum Gravimeter at TCG CREST India

Abhishek Bhardwaj(1), Arijit Sharma(2) and Aishik Acharya(1)
(1) Center for Quantum Engineering, Research and Education; TCG Center for Research and Education in Science and Technology, Kolkata, India
(2) Department of Physics and Center for Atomic, Molecular and Optical Sciences & Technology, Indian Institute of Technology Tirupati, Tirupati, India

Corresponding author's email: *aishik.acharya@gmail.com*

Abstract

At TCG CREST Kolkata, India, we have started the development of an absolute quantum gravimeter (AQG). In this paper, we will describe the present status and the development of a comprehensive physics package and optical setup highlighting its potential for precise gravity measurements with applications in mining, earthquake detection, and navigation. Our experimental setup has three main building blocks namely, sensor head, optical setup, and electronics. The paper provides insights into the status of our research, shedding light on achieved milestones, challenges, and promising outcomes. Additionally, it outlines the roadmap for future work, emphasizing ongoing developments and innovations. This study contributes to the advancement of measurement techniques for acceleration due to gravity, opening avenues for diverse practical applications and paving the way for further advancements in the field of cold atom gravimetry.

1. Introduction

In the realm of precision measurement, atom interferometers have emerged as powerful tools with unparalleled inertial sensitivity. Their capacity for precise gravity measurements surpasses that of conventional instruments, as numerous research studies predict the sensitivity of up to 3×10^{-9} g [1][2]. The LNE-SYRTE portable cold atom gravimeter reportedly has a short-term sensitivity of 5.6×10^{-9} g [3]. Another portable absolute gravimeter built by Muquans reports a long-term sensitivity of less than 10^{-9} g [4]. The implications extend beyond theoretical exploration, offering practical applications such as enhanced mining operations, geophysical prospecting, and environmental monitoring [5][6][7]. This paper contributes to the evolving landscape of gravimetry by presenting a comprehensive physics package description for a cold atom gravimeter. The existing configuration shall be affixed upon an optical table, intended for the execution of atom interferometry as proof of concept. The ultimate objective is to develop a portable gravimeter featuring diminished dimensions, mass, and power consumption. The working principle and physics package is described in Section I. Subsequent parts are concerned with the optics layout and a description of the detection of the relative population of cold atoms with methods to measure gravity. The working principle draws an analogy to the Mach Zehnder interferometer, wherein atoms, rather than photons, undergo interference to generate a distinct interference pattern [8]. The paper concludes by listing several error sources, the methods to reduce the errors, and future plans of the project.

2. Principle of working

The operational principle of the AQG is based on atom interferometry utilizing cold atoms. Since atoms exhibit smaller de Broglie wavelength, the resolution of interference fringes is much larger than for photons thereby increasing the sensitivity. The procedure is initiated by trapping atoms in the magneto-optical trap (MOT) [9], followed by the deactivation of lasers and magnetic fields, allowing the atom cloud to free-fall under the influence of gravity.

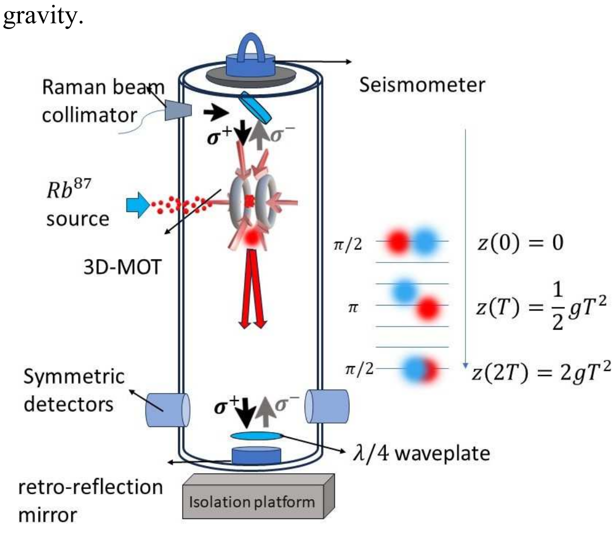

Figure 1. Working principle of gravimeter.

Subsequently, a π/2 pulse is applied, inducing a split into an equal superposition of excited and ground-state atoms. After a duration of time T, a π pulse is employed to invert the state of the two atomic clouds. Conclusively, another π/2 pulse recombines the atoms following an equal time interval T. The entire process is demonstrated in Fig.1. The quantification of atomic populations in ground or excited states occurs within a defined detection region through laser-induced fluorescence, followed by gravity measurement via interference fringe data analysis. This process entails a sequential assembly of procedures, commencing with laser-cooling of atoms to state selection, free fall under gravity with atom interferometry, and concluding with precise detection of the relative population of atoms. All these sub-processes are tightly time synchronized and controlled precisely to perform gravity measurements.

3. Experimental setup

3.1 Physics package

We have a custom-built non-magnetic stainless-steel chamber depicted in Fig. 2 that will be shielded from external magnetic fields by a cylindrical mu-metal shield. We employ a quadrupole magnetic field by utilizing a pair of coils arranged in the anti-Helmholtz configuration. Our simulation results show that 50 turns for each coil with a coil radius of 11 cm will produce a gradient of up to 20 Gauss/cm on the axis with a coil current of 10 A.

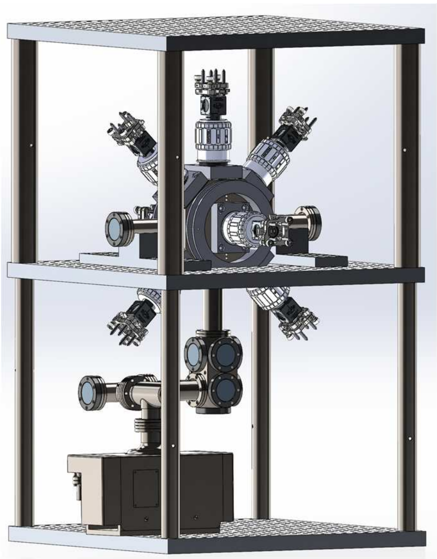

Figure 2. CAD rendering of proposed physics package.

This configuration induces the splitting of Zeeman sub-levels, and it provides a restoring force to the atoms when coupled with laser beams exhibiting σ^+ and σ^- polarization (right and left circularly polarized) [10]. We can simulate two counter-propagating laser beams with $\sigma^+$and σ^- polarization using the pylcp package [11]. The simulation of the force profile experienced by atoms in a MOT can be described by (1).

$$F_{MOT} = -\alpha v - \frac{\alpha\beta}{k} z \quad (1)$$

$$\alpha = 4\hbar k^2 \frac{I}{I_s} \frac{-2\delta/\Gamma}{[1+[2\delta/\Gamma]^2]^2} \quad (2)$$

$$\beta = \frac{g\mu_B}{\hbar} \frac{dB}{dz} \quad (3)$$

The notations used are the same as [12]. The entire process is performed under ultrahigh vacuum (UHV) conditions in a mechanical chamber depicted in Fig. 2 is made of non-magnetic stainless steel. The vacuum level of the order of 10^{-11} torr is maintained using negative high voltage star cell configuration ion pumps.

3.2. Optics layout

Our optical setup generates ten laser beams used to perform the sub-processes as mentioned in previous sections. The laser beams need to be precisely tunable and phase-locked to perform atom interferometry.

We have done laser frequency stabilization by diverting a small power of the laser beam to a glass cell containing ^{87}Rb vapor. [13].

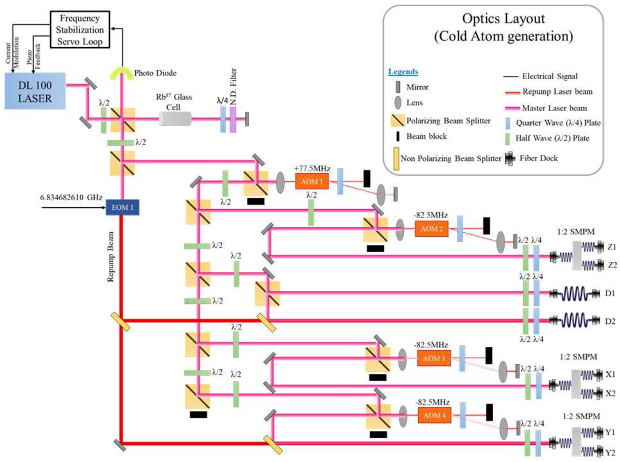

Figure 3. Optics layout for cooling and detection.

In Fig. 3, the comprehensive optical setup for the cooling and detection process is illustrated, portraying the intricate configuration employed in the experiment. The primary laser source undergoes bifurcation, with one segment dedicated to generating the requisite six beams essential for the magneto-optical trap (MOT). The other segment undergoes modulation via an electro-optic modulator (EOM) to serve dual purposes as a re-pumper beam and for the detection region [14]. The creation of the six beams for MOT involves the initial division of the laser into two segments by a beam splitter, with one segment undergoing a double pass configuration through an acousto-optic modulator (AOM) [15]. Replicating this process, utilizing another AOM, results in a detuning of approximately 10 MHz for the MOT laser beams. Subsequently, the beam traverses a polarization-maintaining optical fiber before entering the physics package, ensuring controlled delivery and stability in the experimental setup.

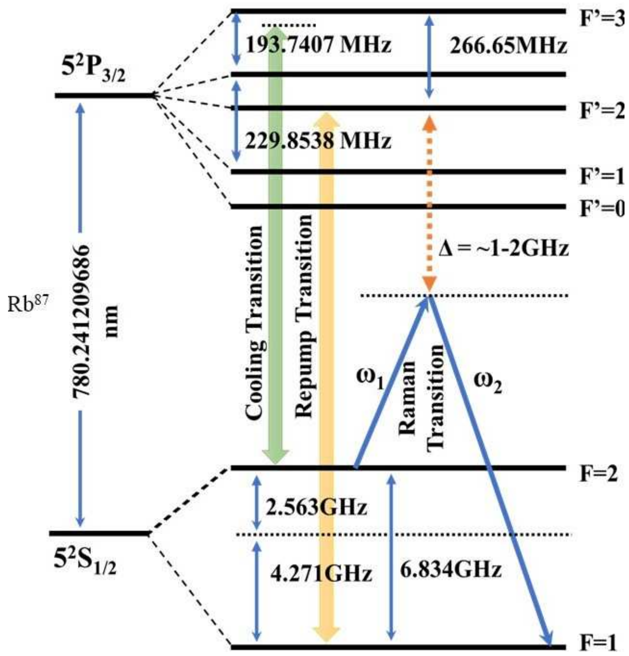

Figure 4. Energy level diagram for ^{87}Rb.

We generate Raman beams through the phase-locking of two lasers. The frequency difference between these beams is crucial, set at 6.834 GHz to enable the desired two-photon Raman transition for an accurate and efficient atom interferometry experiment. [17]

3.3. Detection and measurement of gravity

To extract the signal in atom interferometry the relative the population of the two hyperfine levels $|F=1\rangle$ and $|F=2\rangle$ is measured for ^{87}Rb. As shown in Fig.4 two detection beams are used to measure the fluorescence which can be used to calculate the population of atoms in each state. The upper beam is used to measure and blow away $|F=2\rangle$ state atoms and the lower beam measures the atoms in the state $|F=1\rangle$. The upper beam is σ^+ polarized to drive the closed transition between the levels $|F=2, m_F=2\rangle$ to $|F=3, m_F=3\rangle$. The σ^+ polarized ensures that atoms don't fall to $|F=1\rangle$ dark state [14]. Since the atoms in MOT achieve a certain velocity after they drop, we need to account for the Doppler shift in frequency that is observed by atoms. The time between two Raman pulses is T and the effective wavevector for a single pulse is k_{eff}. If a chirp rate of α MHz/s is applied to the Raman beams, the total phase shift [16] can be shown as-

$$\Delta\phi_{total} = \Delta\phi_{gravity} - \Delta\phi_{Raman} \quad (4)$$

$$\text{Here, } \Delta\phi_{gravity} = k_{eff} g T^2 \ , \quad (5)$$

$$\text{and } \Delta\phi_{Raman} = 2\pi\alpha T^2 \quad (6)$$

When the phase contribution due to chirping of frequency (6) and due to gravity (5) cancels out, we can write g as

$$g = \frac{2\pi\alpha}{k_{eff}} \quad (7)$$

The theoretical calculation of this value, specifically for ^{87}Rb, yields a precise measurement of 25.1 MHz/s. To pinpoint the central fringe accurately, our experimental approach involves manipulating two distinct interrogation times while systematically adjusting the chirp rate. The location of the central fringe peak, where the net phase cancellation occurs, proves consistent across various interrogation times. Subsequently, following the identification of the central fringe, we refine our measurement further. This involves incremental adjustments of the phase of the final $\pi/2$ pulse within the range of 0 to 2π. This procedure allows us to ascertain a more exact and refined value for the chirp rate, as detailed in [17]. Using (7) we can find the precise value of g.

4. Sensitivity and errors

In the realm of measurement, numerous sources of noise pose challenges, with predominant influence from vibrational noise and phase noise within Raman beams. Phase noise, a significant contributor, may arise from the reference source or various optical pathways. To mitigate this, the implementation of a stable phase lock in lasers proves effective in controlling such deviations [18]. Furthermore, the vibrational isolation of retro-reflecting mirrors can be achieved through active damping on the isolation platform [19]. In addressing quantum projection noise effects, a strategic approach involves augmenting the number of trapped atoms, thereby amplifying the amplitude of the detection signal, and concurrently diminishing quantum-related uncertainties [20]. Our current target is to display in-lab sensitivity of the order of a few µGal.

8. Outlook and future plans

Currently, the experimental apparatus has been assembled, and the initial vacuum processing is currently underway. We are baking the system to 200 °C to attain ultrahigh vacuum conditions. The integration of lasers has been accomplished, and their stability has been ensured through the application of saturated absorption spectroscopy targeting the ^{87}Rb transition. Our subsequent objective involves the utilization of a specialized offset frequency locking technique to generate Raman beams. To achieve this, we aim to develop a noise-free signal for input into the EOM and the control of the AOM utilizing our custom-built direct digital synthesis (DDS) system. Additionally, we are working on high-speed sequence generation using an FPGA-based embedded system to control laser frequency, phase, and amplitudes precisely.

9. Acknowledgements

I would like to express my gratitude to my supervisors Dr. Aishik Acharya and Dr. Arijit Sharma for their continued support and guidance in my research activities. I am thankful to Dr. Anju for assisting me with the optical setup. Finally, I would like to thank TCG CREST for the financial support to this project.

References

[1] Ménoret, Vincent, Pierre Vermeulen, Nicolas Le Moigne, Sylvain Bonvalot, Philippe Bouyer, Arnaud Landragin, and Bruno Desruelle. "Gravity measurements below 10− 9 g with a transportable absolute quantum gravimeter." Scientific reports 8, no. 1 (2018): 12300.

[2] Peters, Achim, Keng Yeow Chung, and Steven Chu. "High-precision gravity measurements using atom interferometry." Metrologia 38, no. 1 (2001): 25.

[3] Gillot, Pierre, Bing Cheng, Almazbek Imanaliev, Sébastien Merlet, and F. Pereira Dos Santos. "The LNE-SYRTE cold atom gravimeter." In 2016 European Frequency and Time Forum (EFTF), pp. 1-3. IEEE, 2016.

[4] Ménoret, Vincent, Pierre Vermeulen, Nicolas Le Moigne, Sylvain Bonvalot, Philippe Bouyer, Arnaud Landragin, and Bruno Desruelle. "Gravity measurements below 10− 9 g with a transportable absolute quantum gravimeter." Scientific reports 8, no. 1 (2018): 12300.

[5] B Bidel, Yannick, Olivier Carraz, Renée Charrière, Malo Cadoret, Nassim Zahzam, and Alexandre Bresson. "Compact cold atom gravimeter for field applications." Applied Physics Letters 102, no. 14 (2013).

[6] D'Agostino, Giancarlo, Sergio Desogus, Alessandro Germak, Claudio Origlia, Danilo Quagliotti, Giovanna Berrino, Gennaro Corrado, Vincenzo d'Errico, and Giuseppe Ricciardi. "The new IMGC-02 transportable absolute gravimeter: measurement apparatus and applications in geophysics and volcanology." Annals of Geophysics (2008).

[7] Mickus, Kevin. "Gravity method: environmental and engineering applications." In Department of Geosciences, Southwest Missouri State University, Springfield.

[8] Gustavson, Todd Lyndell. "Precision rotation sensing using atom interferometry." PhD diss., Stanford University, 2000.

[9] Phillips, William D. "Laser cooling and electromagnetic trapping of neutral atoms." In Coherent and Collective Interactions of Particles and Radiation Beams, pp. 209-242. IOS Press, 1996.

[10] Lett, Paul D., William D. Phillips, S. L. Rolston, Carol E. Tanner, R. N. Watts, and C. I. Westbrook. "Optical molasses." *JOSA B* 6, no. 11 (1989): 2084-2107.

[11] Eckel, Stephen, Daniel S. Barker, Eric B. Norrgard, and Julia Scherschligt. "PyLCP: A python package for computing laser cooling physics." Computer physics communications 270 (2022): 108166.

[12] Foot, Christopher J. *Atomic physics*. Vol. 7. OUP Oxford, 2004.

[13] Bowie, Jason, Jack Boyce, and Raymond Chiao. "Saturated-absorption spectroscopy of weak-field Zeeman splittings in rubidium." *JOSA B* 12, no. 10 (1995): 1839-1842.

[14] Tinsley, Jonathan Neil. Construction of a rubidium fountain atomic interferometer for gravity gradiometry. The University of Liverpool (United Kingdom), 2019.

[15] Donley, Elizabeth A., Thomas P. Heavner, Filippo Levi, M. O. Tataw, and Steven R. Jefferts. "Double-pass acousto-optic modulator system." *Review of Scientific Instruments* 76, no. 6 (2005).

[16] McGuirk, Jeffrey Michael. "High precision absolute gravity gradiometry with atom interferometry." PhD diss., Stanford University, 2002.

[17] Kasevich, Mark, and Steven Chu. "Measurement of the gravitational acceleration of an atom with a light-pulse atom interferometer." *Applied Physics B* 54 (1992): 321-332.

[18] Fortier, Fortier, Tara M., David J. Jones, Jun Ye, and Steven T. Cundiff. "Highly phase stable mode-locked lasers." IEEE Journal of Selected Topics in Quantum Electronics 9, no. 4 (2003): 1002-1010.

[19] Yao, Jiamin, Kang Wu, Meiying Guo, Guan Wang, and Lijun Wang. "An ultralow-frequency active vertical vibration isolator with geometric antispring structure for absolute gravimetry." IEEE Transactions on Instrumentation and Measurement 69, no. 6 (2019): 2670-2677.

[20] Gouët, J., T. E. Mehlstäubler, Jaewan Kim, Sébastien Merlet, Andre Clairon, Arnaud Landragin, and F. Pereira Dos Santos. "Limits to the sensitivity of a low noise compact atomic gravimeter." Applied Physics B 92 (2008): 133-144.